

PETROLOGICAL INVESTIGATIONS OF CAIs FROM EFREMOVKA AND NWA 3118 CV3 CHONDRITES. M. A. Ivanova¹, C. A. Lorenz¹, E.V. Korochantseva¹, and G. J. MacPherson². ¹Vernadsky Institute, Kosygin St. 19, Moscow 119991, e-mail: meteorite2000@mail.ru, ivanovama@si.edu; ²Department of Mineral Sciences, National Museum of Natural History, Smithsonian Institution, Washington, DC. 20560, e-mail: MacPhers@si.edu

Introduction: Recent major advances in microanalytical instrumentation have led to a resurgence of interest in Ca-Al-rich inclusions (CAIs), particularly from the point of view of isotopic compositions. Being the first solids to form from the cooling protoplanetary disk during the birth of our solar system [1,2], CAIs record the detailed chronology of high-temperature events during the first 1-2 million years of solar system history. Different types of CAIs record diverse events and histories, and analytical techniques have now improved to the point where it is possible to resolve time differences between those events. Doing so requires comprehensive correlated studies of each individual CAI, including mineralogy, petrology, isotopic compositions and absolute ages. Only the CV3 chondrites contain inclusions of sufficient size to achieve this goal with current technology, and only CAIs from the reduced CV3s are suitably pristine. As part of a new project to develop a large suite of new CAIs for correlated studies, several new big CAIs were extracted from the Efremovka and NWA3118 CV3 chondrites. Here we report preliminary results on mineralogy, petrology and bulk chemistry of two CAIs, 27cE (Efremovka) and 16N (NWA 3118).

Analytical procedure: Polished sections were studied using an FEI Nova NanoSEM 600 scanning electron microscope, equipped with a Thermo Electron energy dispersive X-ray spectrometer. The SEM was operated at 15kV, with a beam current of 2-3 nA. Full-spectrum X-ray image mosaics were collected for each entire inclusion, allowing the bulk composition of the inclusion to be calculated by summing the spectra of all ($\sim 10^{10}$) pixels in the composite image. Minerals were analyzed using a JEOL JXA-8900R electron microprobe at the Smithsonian and a Cameca-SX100 at the Vernadsky Institute.

Results: CAI# 27cE (Fig. 1) is a ~1 cm irregularly-shaped Type B1 inclusion. The mantle is predominantly melilite (crystal size ~1.5 mm) that encloses small euhedral spinel crystals (2-10 μ m) and rare Ca-Al-Ti silicate (15 μ m) grains that are similar in composition to "UNK" [3]. Symplectites of perovskite and melilite occur along outer part of the mantle near where it contacts the Wark-Lovering rim. The core of 27cE is composed of melilite (0.2 mm), pyroxene (0.3 mm), anorthite (0.4 mm), numerous euhedral spinel crystals (2-15 μ m), and sparse FeNi metal

grains. The CAI is surrounded by a ~10 μ m Wark-Lovering rim of pyroxene and melilite with euhedral tiny grains of spinel. The CAI contains no alteration phases. The modal composition of the CAI (vol%): melilite – 69, pyroxene – 10, spinel – 16, anorthite – 5. Melilite varies from Ak₁₄ to Ak₃₃ in the rim, and from Ak₃₁ to Ak₇₀ in the core and the mantle zone (Fig. 2). The primary pyroxene contains 13-21% Al₂O₃ and 3-17% TiO₂ (calc. as Ti⁴⁺) (Fig. 2). The most Ti-rich compositions are higher than typically found in Type B CAI pyroxene [6], although they are similar to some crystals occurring in Type B1 mantles that have been interpreted as relict grains trapped by the CAI parent melts [6]. Pyroxene in the Wark-Lovering rim is relatively depleted in Al₂O₃ and TiO₂, and contains up to 2% FeO. Rim spinel likewise is slightly enriched in FeO. FeNi metal contains (wt%): Ni – 68.7, Co-1.9, V -1.1, P-0.5, Cr-0.3.

CAI#16N (Fig. 1) is a triangular fragment of a Compact Type A inclusion, ~1 cm in original size. The CAI contains coarse (up to 0.2 mm long), tabular melilite crystals, minor subhedral pyroxene grains (up to 0.1 mm in size), small euhedral spinel crystals 5-20 μ m, and minor anorthite (0.07 mm). Minor nepheline and sodalite develop around anorthite grains. Accessory phases include perovskite, 15 μ m-sized Ca-Al-Ti silicate grains (UNK), metal, and small hibonite crystals located just interior to the Wark-Lovering. The rim itself (~20 μ m thick) consists of pyroxene, melilite and spinel. The modal composition of #16N is (vol%): melilite 82, spinel – 7, pyroxene – 9, An – 1.8, hib – 0.2. Melilite crystals exhibit normal zoning from Ak₂₄ outward to Ak₅₆ (Fig. 2). Melilite in the outermost 50 microns of the CAI is more Al-rich than that in the interior (Fig. 1). Interior pyroxene contains 17-24% Al₂O₃ and 7-15% TiO₂ (calc. as Ti⁴⁺) (Fig. 3). Pyroxene in the Wark-Lovering rim is aluminous diopside (Fig. 2). Metal contains (wt%) Ni 3-9, Fe 19-55, and has detectable Os, Pt, Ru, and Mo in varying proportions.

Discussion: The bulk composition (Fig. 3) of # 27cE is somewhat more melilite-rich than is typical for Type B1 CAIs, and plots intermediate between the Types A and B fields, whereas that of #16N is squarely within the Type A field. [4,5]. Both inclusions are very pristine like the ones in the reduced

CV3s, having no (27cE) or only trace amounts (16N) of second alteration, so the compositions as shown in Fig. 3 are accurate representations of their primary bulk compositions.

The composition of #27cE likely indicates that there is a continuum of compositions between Types B and A CAIs, and this in turn demonstrates the need for more high-quality bulk composition data for pristine CAIs. Consistent with previous observations, the composition of the Type A (16N) is close (Fig. 3) to the predictions for equilibrium condensation [7] but that of the Type B (27cE) is not, indicating that “classic” condensation alone cannot account for the bulk compositions of many CAIs. With the eventual addition of approximately 20 new precise bulk compositions to the data set, which will come out of this

project, it will be possible to quantitatively evaluate far better the nature of the compositional deviations of natural CAIs from those of thermodynamic predictions, and thus constrain the process (es) that formed the natural objects

References: [1] MacPherson G. (2003) *In Treatise on Geochemistry*, 1 (ed. A.M. Davis). [2] Krot A et al. (2005) *Nature*, 434, 998. [3] Paque J. et al. (1994) *Meteoritics*, 29, 673-682. [4] Wark D. (1987) *Geochim. Cosmochim. Acta* 51, 221. [5] MacPherson G and Huss G. (2005) *Geochim. Cosmochim. Acta*, 69, 3099. [6] Simon S.B. et al. (1991) *Geochim. Cosmochim. Acta*, 55, 2635-2655 [7] Yoneda S. and Grossman L. (1995) *Geochim. Cosmochim. Acta* 59, 3413.

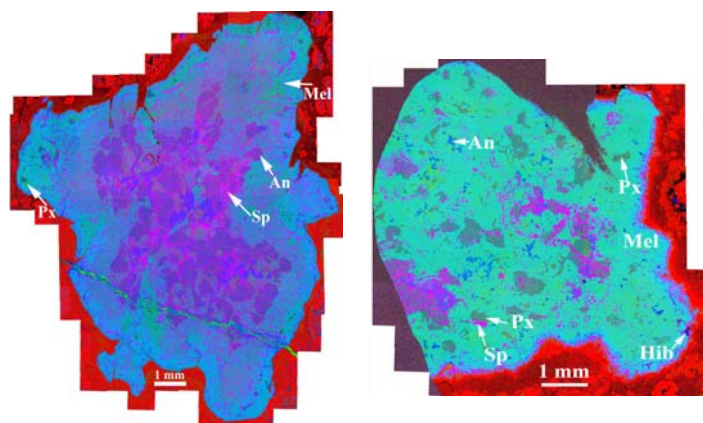


Fig. 1. False color element map of #27cE (left) and #16N (right). Ca = green, Mg = red, Al = blue.

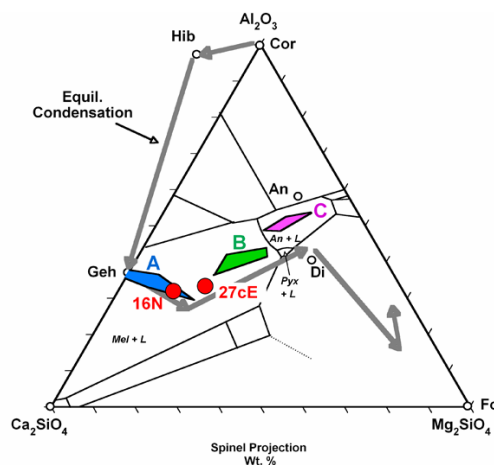


Fig. 3. Bulk compositions of CAIs, with comparison fields for Types A, B, and C. The diagram is from [5]; the condensation trend is from [7].

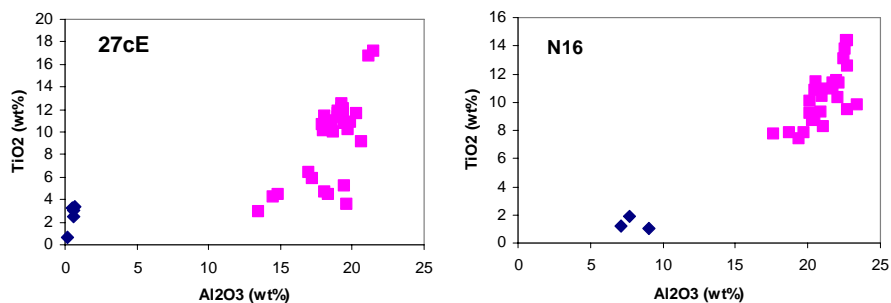


Fig. 2. TiO_2 vs. Al_2O_3 in pyroxene; pink squares – interior. blue diamonds – Wark-Lovering rim